Roles of inter- and intramolecular vibrations and band-hopping crossover in the charge transport in naphthalene crystal

L. J. Wang, Q. Peng, Q. K. Li, and Z. Shuai

Citation: The Journal of Chemical Physics **127**, 044506 (2007); doi: 10.1063/1.2751191
View online: https://doi.org/10.1063/1.2751191
View Table of Contents: http://aip.scitation.org/toc/jcp/127/4
Published by the American Institute of Physics

Roles of inter- and intramolecular vibrations and band-hopping crossover in the charge transport in naphthalene crystal

L. J. Wang, Q. Peng, Q. K. Li, and Z. Shuai[a)]
Key Laboratory of Organic Solids, Beijing National Laboratory for Molecular Sciences (BNLMS), Institute of Chemistry, Chinese Academy of Sciences, 100080 Beijing, People's Republic of China

(Received 20 April 2007; accepted 29 May 2007; published online 27 July 2007)

We calculate the hole and electron mobilities in naphthalene crystal from 10 to 300 K within the framework of the Holstein-Peierls model coupled with first-principles density-functional-theory-projected tight-binding band structures. All the electron-phonon coupling constants, including both local and nonlocal parts for inter- and intramolecular vibrations, have been taken into considerations through density functional theory. The band-hopping crossover transition temperature for the electron transport in the c' axis is calculated to be around 23 K. We have identified a few high frequency intramolecular vibrations which are very important to the charge transport in naphthalene crystal due to their comparatively large electron-phonon coupling constants. However, their contributions to the temperature dependence of mobility are minor because of the small phonon occupations and small nonlocal coupling strengths. The low frequency intermolecular modes (longitudinal optical modes) are found to be the major contributions to the temperature dependent charge transfer properties in naphthalene crystal. Even though the calculated qualitative temperature dependence is in agreement with experiment, the predicted absolute mobility is about one to two orders of magnitude larger. © *2007 American Institute of Physics*.
[DOI: 10.1063/1.2751191]

I. INTRODUCTION

Organic semiconductors have been widely studied in recent years.[1,2] Organic materials have been used in light-emitting diodes, thin-film transistors, and photovoltaic cells. The advantages lie in the mechanical flexibility, large area coverage, and inexpensive mass production in the near future.[3,4] To realize these applications, one of the most important tasks is to improve the charge transport property. Recently, single-crystal organic transistors provide a useful tool to explore and to understand the intrinsic charge transport processes in organic electronic devices.[4] Although rapid progress has been made,[5–12] the fundamental understanding of the charge transport mechanism is still incomplete even for the ultrapure organic crystals.

Charge transport can be classified into two different types, band model[5–8] and hopping model.[9–12] At low temperatures, coherent bandlike transport of delocalized carriers is believed to be the dominant transport mechanism in single crystals. The mobility decreases with temperature because the lattice vibrations scatter the carriers. At high temperatures, transport occurs by hopping of charges between localized states, where transport is phonon assisted, so the charge mobility increases with temperature. The transition between band and hopping mechanisms in organic crystals was first observed in naphthalene crystal.[13] Even though great efforts[7,8,14–19] have been spent on studying the conductivity in naphthalene crystal, a clear understanding in terms of molecular vibration contributions to the anisotropy and band-hopping transition is still limited. In addition, we are interested in answering the following question: Is it possible to predict the transport properties for organic solids from first principles?

A useful model to describe the charge transport in organic materials is based on the small-polaron theory proposed by Holstein[5] for polaron motion in a one-dimensional molecular crystal, within which a single excess charge carrier is contained. After applying a number of simplifications, the zeroth order adiabatic treatment of the polaron problem was developed. Kenkre *et al.*[7] assumed directionally dependent local coupling constants and obtained the Holstein-type mobility expression which can be applied to fit the measured electron mobilities reasonably well. They gave the first explanation of the mobility behavior in naphthalene crystal. Nonlocal couplings were also considered in more generalized polaron methods. Munn and Silbey[6] suggested a variational theory, which contained both local and nonlocal linear electron-phonon couplings. They found that nonlocal couplings increase the scattering, which give lower band contributions and higher hopping contributions. Recently, Hannewald and Bobbert[8,17] have generalized the Holstein model to the Holstein-Peierls model by including nonlocal electron-phonon couplings with parameters calculated at the *ab initio* level. Their investigations on naphthalene crystal were in qualitative agreement with the experiment in terms of temperature dependence.[8] The temperature dependences for electron and hole mobility as well as the spatial anisotropy behaviors have been obtained by taking only three intermolecular vibration/rotation modes into considerations.

In this paper, we start with the Holstein-Peierls model, and we focus on the roles of inter- and intramolecular cou-

a)Electronic mail: zgshuai@iccas.ac.cn

plings, calculated from first principles, to investigate carrier mobility, for the temperature dependence and the anisotropy as well as the band-hopping transition in naphthalene crystal. The contributions from inter- and intramolecular vibrations and the local and nonlocal electron-phonon couplings are analyzed in full detail in order to give a comprehensive description for the charge transport process in organic crystals.

II. THEORETICAL METHODOLOGY

A. Model

The Holstein-Peierls model reads

$$H = H_e + H_p + H_{e\text{-}p} = \sum_{mn} \varepsilon_{mn} a_m^+ a_n + \sum_{\lambda} \hbar\omega_\lambda \left(b_\lambda^+ b_\lambda + \frac{1}{2}\right) + \sum_{mn\lambda} \hbar\omega_\lambda g_{\lambda mn} (b_\lambda^+ + b_{-\lambda}) a_m^+ a_n. \quad (1)$$

Here, the Hamiltonian contains the electronic part (H_e), the phonon part (H_p), and the electron-phonon coupling part ($H_{e\text{-}p}$). The operators $a_m^{(+)}$ and $b_\lambda^{(+)}$ represent annihilating (creating) an electron at the lattice site m with energy ε_{mm} and a phonon belonging to mode λ with frequency ω_λ, respectively. $g_{\lambda mn}$ is the dimensionless electron-phonon coupling constant.

The Hamiltonian was canonically transformed into polaron plus distorted phonon by using a unitary transformation.[7,17,20] Then, the conductivity can be evaluated with the Kubo formalism for linear response theory with a current-current correlation function.[21] After some approximations and complex derivations,[17,20] Hannewald *et al.* have worked out the mobility formula within the framework of the Holstein-Peierls model, which is qualitatively similar to the expression[7] of Kenre *et al.* due to the Holstein model. The mobility can be expressed as

$$\mu_\alpha(T) = \frac{e_0}{2k_B T\hbar^2} \sum_{n\neq m} R_{amn}^2 \int_{-\infty}^{\infty} dt e^{-\Gamma^2 t^2} \left[\varepsilon_{mn}^2 + (\varepsilon_{mn} - \Delta_{mn})^2 + \frac{1}{2}\sum_q (\hbar\omega_q g_{qmn})^2 \Phi_q(t) \right] e^{-2\Sigma_\lambda G_\lambda [1+2N_\lambda - \Phi_\lambda(t)]}, \quad (2)$$

where $\Delta_{mn} = \frac{1}{2}\Sigma_\lambda \hbar\omega_\lambda \left[g_{\lambda mn}(g_{\lambda mm} + g_{\lambda nn}) + \frac{1}{2}\Sigma_{k\neq m,n} g_{\lambda mk} g_{\lambda kn} \right]$. $R_{\alpha mn}$ is the distance between lattice sites m and n in the α direction. $G_\lambda = g_{\lambda mm}^2 + \frac{1}{2}\Sigma_{k\neq m} g_{\lambda mk}^2$ is the effective coupling constant of mode λ, which includes both the local and nonlocal parts. $N_\lambda = 1/(e^{\hbar\omega_\lambda/k_B T} - 1)$ is the phonon occupation number of mode λ. The time dependent quantity $\Phi_q(t) = (1+N_q)e^{-i\omega_q t} + N_q e^{i\omega_q t}$ describes the incoherent scattering events caused by phonon number changes, and the factor $e^{-2\Sigma_\lambda G_\lambda[1+2N_\lambda]}$ in Eq. (2) represents the bandwidth narrowing.[8,20] Γ is a phenomenological parameter for inhomogenous line broadening.

In order to understand the temperature dependence of mobility, we separate the local and nonlocal contributions to the mobility according to Eq. (2) by defining

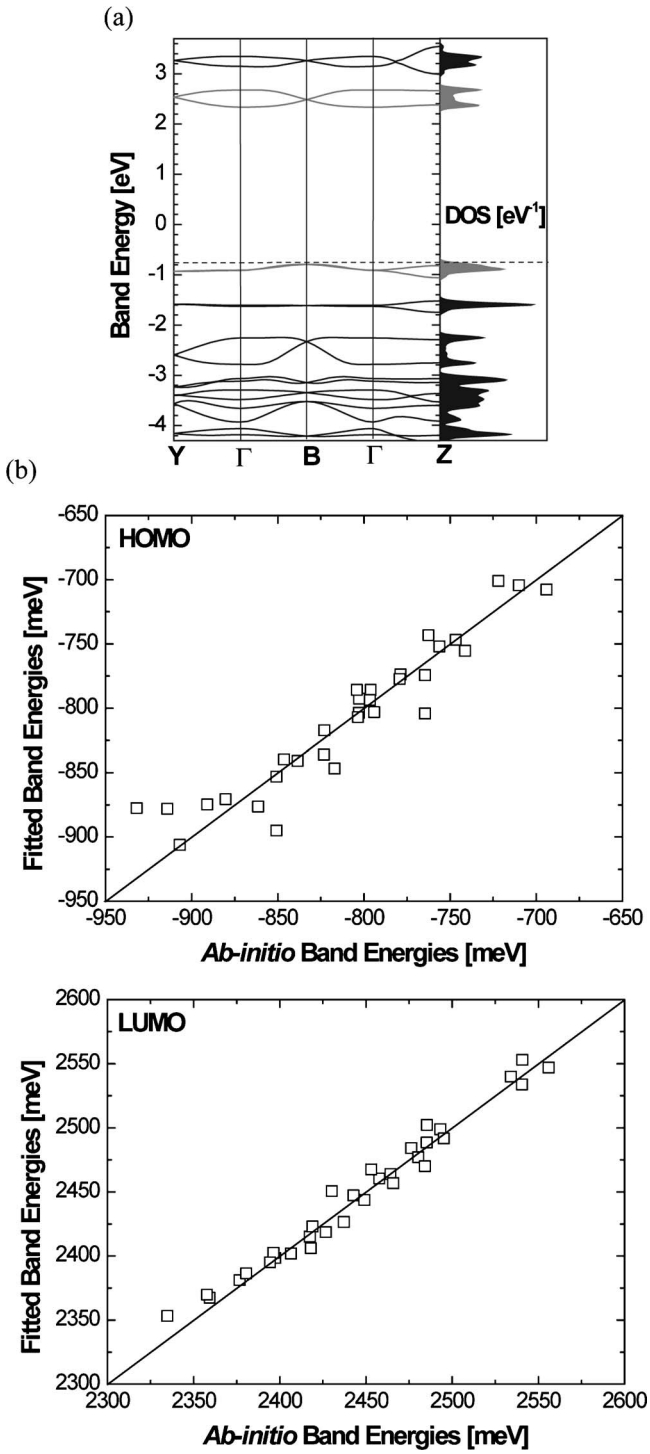

FIG. 1. (a) DFT/PBE calculated band structure. The high-symmetry points in units of $(2\pi/a, 2\pi/b, 2\pi/c)$ are $\Gamma=(0,0,0)$, $Y=(0.5,0,0)$, $B=(0,0.5,0)$, and $Z=(0,0,0.5)$; (b) comparison of the DFT-calculated and the fitted tight-binding band energies for 64 selected k points.

$$\mu_\alpha(T) = A_\alpha f(T) + \sum_q B_{\alpha q} h_q(T), \quad (3)$$

where

$$A_\alpha \equiv \frac{e_0}{2k_B\hbar^2} \sum_{n\neq m} R_{amn}^2 [\varepsilon_{mn}^2 + (\varepsilon_{mn} - \Delta_{mn})^2],$$

TABLE I. First-principles-mapped tight-binding model: on-site energies, transfer integrals, and the electron-phonon coupling constants for the most important 13 phonons.

		0	*a*	*b*	*c*	*ac*	*ab*	*abc*
HOMO	t_{mn} (meV)	−835	−23	−42	−3	−1	22	−5
	g_{1mn}	−0.27	−0.09	0.49	0.13	0.13	−0.12	0.08
	g_{2mn}	0.15	−0.29	−0.13	0.19	0.05	−0.02	0.08
	g_{3mn}	−0.08	0.03	−0.12	0.03	0.08	−0.19	0.03
	g_{4mn}	0.00	0.00	0.01	0.00	0.00	−0.01	0.00
	g_{5mn}	0.05	0.02	−0.06	−0.02	−0.03	0.05	−0.03
	g_{6mn}	−0.05	0.00	−0.02	0.00	0.00	−0.01	0.00
	g_{7mn}	−0.21	−0.01	0.00	0.01	0.00	0.01	0.00
	g_{8mn}	0.06	0.02	0.03	0.00	0.00	−0.02	0.00
	g_{9mn}	−0.15	−0.01	−0.01	0.00	0.00	0.00	0.00
	g_{10mn}	0.32	0.00	0.00	0.00	0.00	0.00	0.00
	g_{11mn}	−0.10	0.00	0.00	0.00	0.00	0.01	0.00
	g_{12mn}	0.10	0.00	0.01	0.00	0.00	0.00	0.00
	g_{13mn}	0.24	0.00	−0.01	0.00	0.00	0.00	0.00
LUMO	t_{mn} (meV)	2510	7	24	−3	−1	−51	−2
	g_{1mn}	−0.23	−0.04	−1.31	−0.31	0.01	0.39	0.00
	g_{2mn}	0.19	−0.04	0.20	0.66	−0.11	−0.86	0.10
	g_{3mn}	−0.09	−0.03	0.03	0.13	0.04	0.11	0.03
	g_{4mn}	0.10	0.01	−0.01	0.01	−0.01	−0.03	0.00
	g_{5mn}	−0.10	−0.01	0.04	−0.01	0.01	0.04	0.00
	g_{6mn}	0.15	0.01	0.01	−0.01	0.00	0.00	0.00
	g_{7mn}	0.49	0.00	0.00	0.01	0.00	0.01	0.00
	g_{8mn}	0.10	0.00	−0.02	0.00	0.00	0.00	0.00
	g_{9mn}	0.16	0.00	0.01	0.00	0.00	0.00	0.00
	g_{10mn}	−0.41	0.00	0.00	0.00	0.00	0.00	0.00
	g_{11mn}	0.06	0.00	0.00	0.00	0.00	0.00	0.00
	g_{12mn}	−0.05	0.00	0.00	0.00	0.00	0.00	0.00
	g_{13mn}	−0.16	0.00	0.01	0.00	0.00	−0.01	0.00

$$B_{\alpha q} \equiv \frac{e_0}{2k_B\hbar^2} \sum_{n\neq m} R_{amn}^2 \tfrac{1}{2}\hbar^2\omega_{q8}^2 g_{qmn}^2,$$

$$f(T) \equiv \frac{1}{T}\int_{-\infty}^{\infty} dt e^{\Sigma_\lambda -2G_\lambda(1+2N_\lambda(T))(1-\cos\,\omega_\lambda t)-\Gamma^2 t^2} \times\cos\left(\sum_\lambda 2G_\lambda \sin\,\omega_\lambda t\right),$$

$$h_q(T) \equiv \frac{1}{T}(1+N_q(T))\int_{-\infty}^{\infty} dt e^{\Sigma_\lambda -2G_\lambda(1+2N_\lambda(T))(1-\cos\,\omega_\lambda t)-\Gamma^2 t^2} \times\cos\left(\sum_\lambda 2G_\lambda \sin\,\omega_\lambda t+\omega_q t\right) + \frac{1}{T}N_q(T)\int_{-\infty}^{\infty} dt e^{\Sigma_\lambda -2G_\lambda(1+2N_\lambda(T))(1-\cos\,\omega_\lambda t)-\Gamma^2 t^2} \times\cos\left(\sum_\lambda 2G_\lambda \sin\,\omega_\lambda t-\omega_q t\right).$$

Now, the mobility is expressed as a linear combination of temperature dependent functions. The A_α contains the local contribution and $B_{\alpha q}$ belongs to the nonlocal contribution (g_{mn} term, $m\neq n$). If we leave the common $1/T$ factor aside, the T dependences of $f(T)$ and $h_q(T)$ are through the phonon occupation number $N_q(T)$. $f(T)$ decreases with $N_q(T)$, while $h_q(T)$ has complex T dependence due to an additional multiplicative factor $N_q(T)$. Different parameters of A_α and $B_{\alpha q}$ can cause different T dependent mobilities in different directions.

From another point of view, the mobility can be divided into several parts according to electron-phonon couplings. Since all the T dependent functions depend on the effective coupling constants G_λ which contain both the local and nonlocal coupling constants, we focus on the coefficients A_α and $B_{\alpha q}$ which only contain some of the couplings $g_{\lambda mn}$. The first part of the total mobility is $A_\alpha f(T)$, and the coefficient A_α does not contain any electron-phonon coupling constant. The second part is $\Sigma_q B_{\alpha q} h_q(T)$ (q belongs to all the intermolecular vibrations), and the coefficients $B_{\alpha q}$ only contain the nonlocal couplings of intermolecular phonons. The third is $\Sigma_q B_{\alpha q} h_q(T)$ (q belongs to all the intramolecular vibrations), and the coefficients $B_{\alpha q}$ only contain the nonlocal couplings of intramolecular phonons. We name these three parts as the local part, the nonlocal-inter part, and the nonlocal-intra part, respectively. The detailed contributions of the three different parts to the mobility can give a better understanding of charge transport in ultrapure crystals.

B. Transfer integrals

A number of computational methods,[12,18,20,22–24] including direct "dimer methods" and crystal band-fitting method, have been developed to estimate the transfer integrals. One

of the dimer methods was proposed by Fujita *et al.* in modeling scanning tunneling microscopy.[24] Later, Troisi and Orlandi applied this approach to calculate the transfer integrals in DNA (Ref. 25) and pentacene crystal.[12] The transfer integrals in this scheme can be written as

$$t_{ij} = \langle \Phi_i | F | \Phi_j \rangle, \tag{4}$$

where Φ_i and Φ_j are the unperturbed highest occupied molecular orbitals/lowest unoccupied molecular orbitals (HOMOs/LUMOs) of the two distinct dimers and F is the Fock operator of the system using unperturbed density matrix.[12] It has been employed to study the carrier transport in siloles[26(a)] and triphenylamine dimers.[26(b)] Another direct method was suggested by Senthikumar *et al.*[27] to study the absolute rates of hole transfer in DNA. Recently, Valeev *et al.* have used it to study the effect of electronic polarization on charge transport parameters.[23] The transfer integrals can be written as

$$t_{ij} = \frac{t_{ij}^0 - (1/2)(e_i + e_j)S_{ij}}{1 - S_{ij}^2}. \tag{5}$$

Here, $e_i = \langle \Phi_i | H | \Phi_i \rangle$, $t_{ij}^0 = \langle \Phi_i | H | \Phi_j \rangle$, and $S_{ij} = \langle \Phi_i | S | \Phi_j \rangle$, where H and S are the system Hamiltonian and overlap matrices, respectively.

Another useful method to calculate the transfer integrals is the band-fitting method which is based on the tight-binding model. The solution of this model $\varepsilon(\mathbf{k}) = \varepsilon_0 + \sum_{\langle ij \rangle} \varepsilon_{ij} e^{-i\mathbf{k}\cdot\mathbf{R}_{ij}}$ is a $\mathbf{k}$ dependent function with several adjacent transfer integrals as parameters. Therefore, we can calculate the transfer integrals by fitting the energy bands to the tight-binding-type function. This method is especially useful in evaluating the electron-phonon coupling constants consistently in the same band-structure framework.

In this work, the first-principles density functional theory (DFT) band structure is projected to a tight-binding model by fitting the HOMO and the LUMO energy bands to obtain the most important transfer integrals and electron-phonon coupling constants.[20] The fitting results are sensitive to the nearest neighbors chosen in the tight-binding model. We sort the neighboring dimers according to the distances, and we use the two direct methods described above to calculate the electron couplings between these dimers. Finally, the tight-binding model is set up according to the most electronic couplings evaluated from the dimer method for the band-fitting process.

C. Electron-phonon coupling constants

With the DFT optimized molecular crystal structure, the phonon spectra can be obtained. At the Γ point of phonon band, we (i) displace slightly the molecules according to each normal mode, (ii) carry out another band-structure calculation thereafter, (iii) then fit the transfer integrals ε_{mn}, and (iv) finally the electron-phonon coupling constants can be obtained by numerical differentiation $g_{\lambda mn} = (1/\omega_\lambda \sqrt{\hbar\omega_\lambda}) \times (\partial \varepsilon_{mn}/\partial Q_\lambda)$, where Q_λ is the normal coordinate of phonon λ. The effective coupling constant of mode λ can be evaluated by the format $G_\lambda = g_{\lambda mn}^2 + \frac{1}{2}\Sigma_{k\neq m} g_{\lambda mk}^2$. The total effective charge-carrier–phonon coupling constant is the sum of the effective coupling constants of all the phonons: $G_{\text{tot}} = \Sigma_\lambda G_\lambda$. Therefore, the total effective coupling constant can be expressed as the sum of four parts.

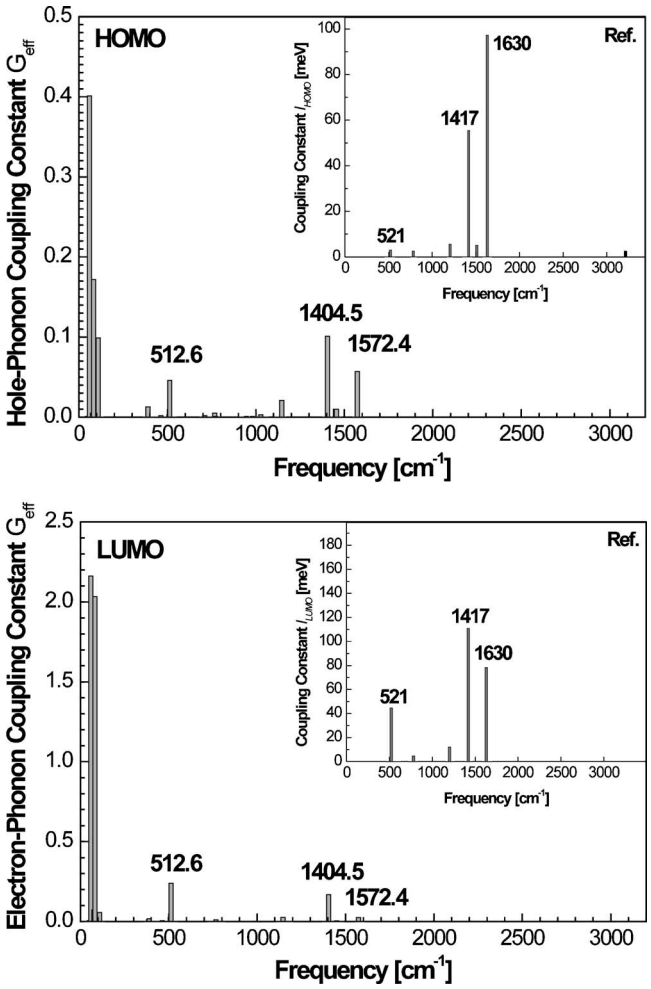

FIG. 2. Effective coupling constants vs phonon energies for HOMO and LUMO. The previous calculations for single naphthalene molecule by Kato and Yamabe (Ref. 14) are shown in the insets.

$$G_{\text{tot}} = \sum_{\lambda \in \text{inter}} g_{\lambda mm}^2 + \frac{1}{2} \sum_{\substack{k\neq m \\ \lambda \in \text{inter}}} g_{\lambda mk}^2 + \sum_{\lambda \in \text{intra}} g_{\lambda mm}^2 + \frac{1}{2} \sum_{\substack{k\neq m \\ \lambda \in \text{intra}}} g_{\lambda mk}^2$$

$$= G_{\text{inter-local}} + G_{\text{inter-nonlocal}} + G_{\text{intra-local}} + G_{\text{intra-nonlocal}}. \tag{6}$$

We are interested in how these terms contribute to the mobility.

III. NUMERICAL RESULTS

A. Calculation details

The Vienna *ab initio* simulation package (VASP),[28] which uses pseudopotential and a plane wave basis set, has proved to be a very useful tool for theoretical study of periodic systems such as crystalline solids.[20,29] In this paper, we fix the

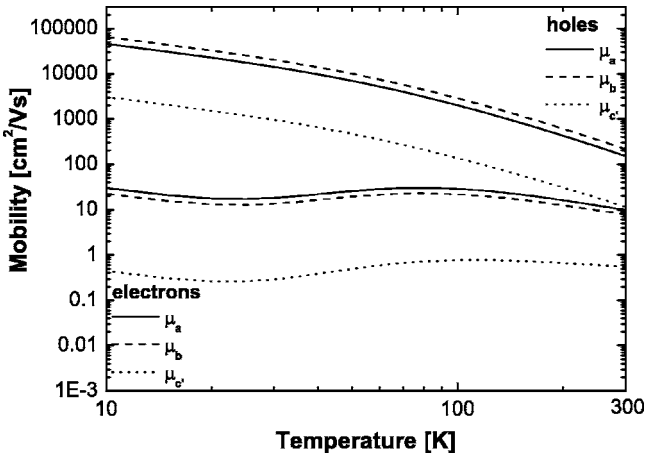

FIG. 3. Calculated charge-carrier mobilities as a function of temperature in naphthalene crystal from 10 to 300 K. (The top three curves are for holes and the rest are for electrons.)

lattice vectors, optimize the crystal, and then calculate the vibrational properties by the VASP code. The Perdew-Burke-Ernzerhof (PBE) exchange-correlation (XC) functional[30] is chosen because it has been found to work better for molecular crystals than other functionals.[31] The initial lattice parameters for naphthalene crystal are $a=8.098$ Å, $b=5.953$ Å, $c=8.652$ Å, $\alpha=\gamma=90°$, and $\beta=124.4°$ according to the Cambridge Structural Database.[32] The threshold for convergence in the total energy of the self-consistent field is 10^{-5} eV, and the atomic forces for the relaxed structure are smaller than 0.01 eV/Å. Force constants are calculated as the numerical derivatives of the atomic forces with respect to atomic displacements, and the phonon frequencies are evaluated with only Γ point. Only optical phonons are considered. A $4\times4\times4$ grid in the corresponding Brillouin zone is used to fit the transfer integrals by a least-squares minimization.

B. Transfer integral evaluation

To calculate the transfer integrals by the band-fitting method, it is essential to decide which neighboring molecule pairs[20] should be included. First, an arbitrary molecule can be chosen as reference since the sit energies for type α and type β molecules in naphthalene crystal are the same due to its monoclinic $P2_1/a$ symmetry.[16] Then the neighboring molecules can be sorted according to their distances to the reference molecule, and the transfer integrals are evaluated by the direct dimer methods. At last, the relationship between the absolute values of the transfer integrals and the index of the neighbors is obtained. The two dimer methods give very close results with the biggest difference of 7.8 meV in deal-

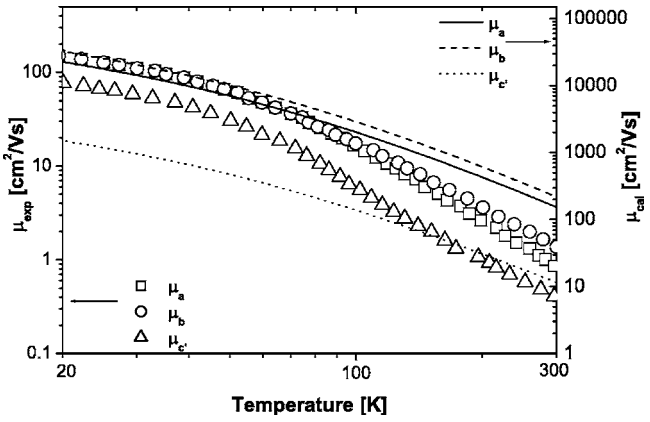

FIG. 4. The hole mobilities vs temperature obtained by calculation and experiment (Refs. 34 and 35) in a, b, and c' directions.

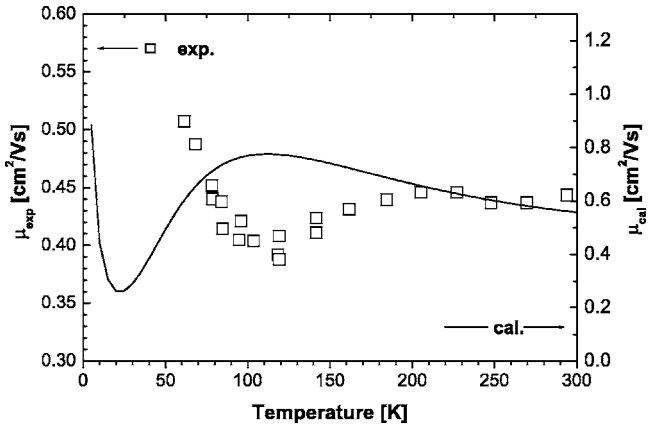

FIG. 5. The band-hopping transition for electron transport in the c' direction: theory versus experiment (Ref. 13).

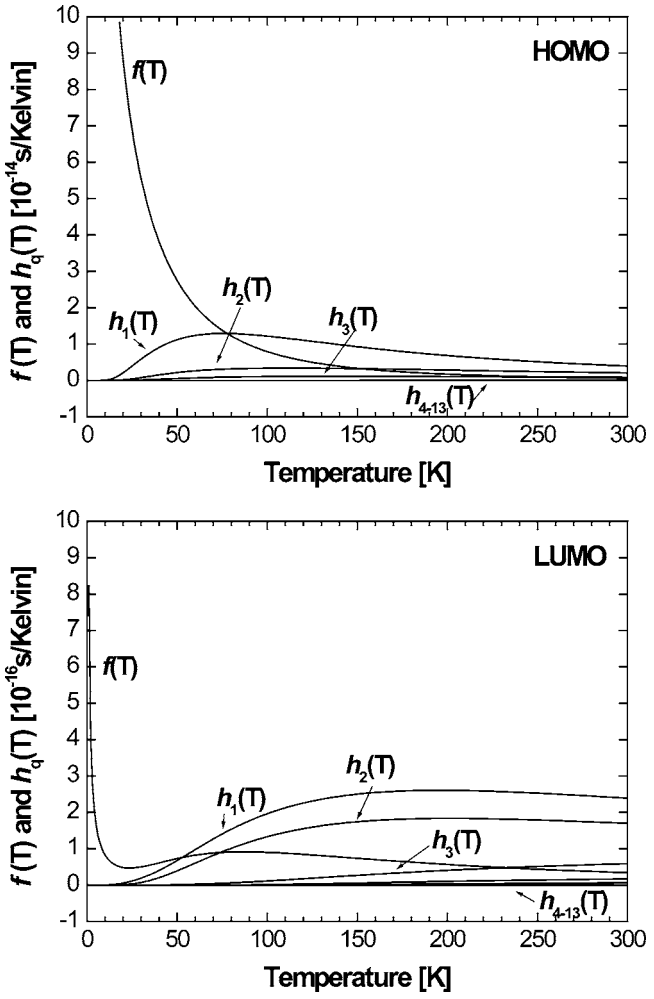

FIG. 6. The calculated temperature dependent functions $f(T)$ and $h_q(T)$ for HOMO and LUMO.

TABLE II. Information of the most important 13 phonon modes, including the phonon energies, effective coupling constants of HOMO and LUMO, and phonon occupation numbers at 10, 150, and 300 K.

				$N_q(T)$		
	$\hbar\omega_q$ (cm^{-1})	G_{eff} (HOMO)	G_{eff} (LUMO)	10 K	150 K	300 K
Intermolecular vibrations	58.8	0.40	2.16	2.12*E*−04	1.320	3.070
	82.0	0.17	2.03	7.57*E*−06	0.837	2.077
	108.5	0.10	0.06	1.67*E*−07	0.546	1.466
Intramolecular vibrations	384.8	0.00	0.01	9.28*E*−25	0.026	0.188
	388.9	0.01	0.02	5.12*E*−25	0.025	0.183
	507.6	0.00	0.02	1.98*E*−32	0.008	0.096
	512.6	0.05	0.24	9.55*E*−33	0.007	0.094
	767.1	0.01	0.01	1.22*E*−48	6.40*E*−04	0.026
	1145.6	0.02	0.03	2.78*E*−72	1.70*E*−05	0.004
	1404.5	0.10	0.17	1.88*E*−88	1.42*E*−06	0.001
	1449.7	0.01	0.00	2.81*E*−91	9.19*E*−07	9.60*E*−04
	1454.3	0.01	0.00	1.44*E*−91	8.79*E*−07	9.38*E*−04
	1572.4	0.06	0.02	6.12*E*−99	2.83*E*−07	5.33*E*−04

ing with the same dimer; therefore, either of the dimer methods can be used to determine which neighbors should be considered in the band fit. We choose all the nearest neighbors and the molecules with large transfer integral calculated by the dimer methods. Therefore, six neighbors[20] are chosen for band fitting, i.e., $\{mn\}=\{0,a,b,c,ac,ab,abc\}$ belonging to $\boldsymbol{R}_{mn}=0$, $\pm\boldsymbol{a}$, $\pm\boldsymbol{b}$, $\pm\boldsymbol{c}$, $\pm(\boldsymbol{a}+\boldsymbol{c})$, $\pm(\boldsymbol{a}/2\pm\boldsymbol{b}/2)$, $\pm(\boldsymbol{a}/2\pm\boldsymbol{b}/2+\boldsymbol{c})$. We show the calculated energy band in Fig. 1(a), which is identical to Hummer and Ambrosch-Draxl's calculations.[19] In Fig. 1(b), we compare the band energies of HOMO and LUMO for the chosen $4\times4\times4$ grid obtained by both the *ab initio* calculations and the band-fitting method. We can see that the fitted band energies are in good agreement with the *ab initio* calculated results. The transfer integrals are listed in Table I. Again the values are consistent with Hannewald *et al.*[20] and the slight differences come from the different initial crystal structures and exchange-correlation functionals.

C. Electron-phonon coupling constants

The relationship between the coupling constants and the phonon energies is plotted in Fig. 2. At a first glance, the low frequency phonon couplings are much larger than high frequency phonons, especially for LUMO. However, we can also find that some intramolecular phonons seem to be important. Their frequencies are 512.6, 1404.5, and 1572.4 cm^{-1}, which are in good agreement with Kato and Yamabe's calculations (see Fig. 2 and its insets) for naphthalene molecule.[14] Namely, the crystal dispersion effect is minor. In Table I, we list the most important 13 modes with effective coupling constants larger than 0.01 for HOMO and LUMO. The effective coupling constants of the first three phonons are very close to the results of Hannewald *et al.* within the rigid-molecule approximation.[20]

D. Mobility calculation

The dominant scattering sources in organic crystals are optical phonons, acoustic phonons, and static impurities.[33] The optical phonon scatterings have been considered in Eq. (2), while the effects of acoustic phonons are neglected.[8] Since we focus on the conductivity in ultrapure crystals, a very small value must be chosen for the inhomogeneous broadening factor ($\hbar\Gamma$) which is caused by impurity and does not depend on the temperature.[8] Therefore, $\hbar\Gamma=0.1$ meV has been chosen in the present calculations. The contribution of acoustic phonon remains a challenge.

In Fig. 3, we present the calculated electron and hole mobilities in naphthalene crystal as a function of temperature in a, b, and c' directions. Here, c' is perpendicular to the ab plane of naphthalene crystal. The temperature dependence of the calculated mobilities generally agrees well with Karl's experimental works[34,35] except for a and b directions of electrons. The disagreement of these two directions can be due to the overestimated electron-phonon coupling constants of electrons related to the difficulties of DFT in describing weak van der Waals interaction. Our calculations in these two directions differ from Ref. 8 since we constrain the lattice vectors to the experimental values in the optimization[36] and use PBE XC functional[31] in calculating the electron-phonon coupling constants. From Fig. 4, we can find that our calculated temperature dependences of hole mobilities are in very good agreement with the experiment below 60 K. At higher temperatures, the theoretical results show a slower decrease. This is due to the approximation in this work that the canonically transformed transfer integrals are replaced by their thermal average,[17] which smeared out the thermal fluctuation contribution.[12] The calculated and the experimental electron mobilities in the c' direction are presented in Fig. 5. The band-hopping transition can be clearly seen. However, the band-hopping transition temperature is calculated to around 23 K, which is smaller than the experimentally measured 100–150 K range. According to Silbey and Munn,[37] the larger the electron-phonon coupling, the lower the transition temperature. It is likely that the coupling between the electron and the intermolecular coupling is overestimated in the present approach. Even though PBE functional is so far

TABLE III. The calculated coefficients A and B_q for HOMO and LUMO in the a, b, and c' directions (the unit is $cm^2\,K/V\,s^2$).

	HOMO			LUMO		
	a	b	c'	a	b	c'
A	2.66*E*17	3.80*E*17	1.78*E*16	4.53*E*17	3.37*E*17	6.62*E*15
B_1	1.11*E*14	6.44*E*14	1.69*E*14	5.14*E*14	4.53*E*15	3.40*E*14
B_2	8.63*E*14	9.41*E*13	3.64*E*14	4.85*E*15	2.05*E*15	3.28*E*15
B_3	3.08*E*14	2.68*E*14	1.02*E*14	2.28*E*14	6.62*E*13	2.62*E*14
B_4	8.40*E*12	1.83*E*13	5.13*E*12	1.08*E*14	6.27*E*13	1.32*E*13
B_5	3.73*E*14	5.23*E*14	3.76*E*14	2.36*E*14	2.92*E*14	3.87*E*13
B_6	8.80*E*12	5.78*E*13	2.97*E*12	3.60*E*13	5.64*E*12	1.38*E*13
B_7	4.85*E*13	4.12*E*12	2.76*E*13	1.93*E*13	1.09*E*13	8.55*E*12
B_8	5.46*E*14	4.90*E*14	1.23*E*13	1.26*E*13	1.58*E*14	2.04*E*13
B_9	6.13*E*13	3.16*E*13	6.89*E*12	4.67*E*13	2.59*E*13	4.41*E*13
B_{10}	4.41*E*12	2.16*E*12	2.07*E*12	2.63*E*13	7.20*E*12	6.21*E*12
B_{11}	8.38*E*13	3.99*E*13	1.54*E*13	1.61*E*13	2.07*E*13	2.21*E*12
B_{12}	3.74*E*13	4.24*E*13	2.22*E*13	2.62*E*13	1.47*E*13	6.66*E*12
B_{13}	2.47*E*13	1.55*E*14	3.89*E*13	1.59*E*14	3.82*E*14	6.49*E*13

one of the most reliable approaches to deal with weak interaction, more elaborate electronic structure theory for van der Waals interaction is in demand.

E. Temperature dependence

In order to reveal the temperature dependence behavior, we plot the functions $f(T)$ and $h_q(T)$ in Fig. 6, from which three observations can be made. First, $f(T)$ for HOMO and for LUMO are slightly different because of the difference in electron-phonon and hole-phonon coupling strengths. As shown in Tables I and II, the hole-phonon coupling (for HOMO) is weak, while the electron-phonon coupling (for LUMO) is quite strong. Therefore, $f(T)$ for HOMO decreases monotonically and rapidly with temperature, while for LUMO, after a sharp decrease, it becomes quite flat and shows a shallow minimum already at low temperature. The $f(T)$ behaviors arising from the local linear electron-phonon coupling are in good agreement with what have been found by Silbey and Munn.[37] Secondly, we find that the functions $h_q(T)$ increase first and then level off, and finally decrease with temperature, which is very different from $f(T)$. Thirdly, $h_q(T)$ decreases rapidly with the energy of the phonons. The lowest three modes $(q=1,2,3)$ from the intermolecular vibrations are much larger than the rest of $h_q(T)$. In brief, the bandlike picture comes from the $f(T)$, while the hopping behaviors are mainly from $h_q(T)$. In principle, the linear combination of the two terms allows a comprehensive description of band-hopping crossover. The coefficients come from first-principles calculations.

The calculated coefficients A and B_q are given in Table III. First, let us consider the hole transport. All of the coefficients B_q for HOMO are ranging from 10^{12} to 10^{14} (in $cm^2\,K/V\,s^2$), which are much smaller than the coefficients A which fall in the range of 10^{16}–10^{17} (in $cm^2\,K/V\,s^2$) for all the Cartesian directions. Therefore, the hole mobilities are mainly determined by the bandlike function $f(T)$. Consequently, the hole mobilities in all the three directions have very similar temperature dependences (see Fig. 4). Secondly, for electron transport, in both a and b directions for LUMO, the coefficients A are much larger than the coefficients B_q. However, in the c' direction, the coefficient A is close in value to some of the coefficients B_q. Moreover, this indicates that the band-hopping crossover could happen in the electron transport in the c' direction for naphthalene crystal. Indeed, from our first-principles calculations, this interesting behavior is manifested (see Fig. 5).

TABLE IV. The hole (HOMO) and electron (LUMO) mobility decompositions into local, nonlocal-inter, and nonlocal-intra parts at $T=10$ and 300 K.

		Local part		Nonlocal-inter part		Nonlocal-intra part	
		10 K	300 K	10 K	300 K	10 K	300 K
HOMO	a	100.00%	98.51%	0.00%	1.48%	0.00%	0.01%
	b	100.00%	98.74%	0.00%	1.25%	0.00%	0.01%
	c'	100.00%	87.91%	0.00%	11.99%	0.00%	0.10%
LUMO	a	100.00%	94.14%	0.00%	5.83%	0.00%	0.03%
	b	100.00%	88.88%	0.00%	11.07%	0.00%	0.05%
	c'	99.99%	25.71%	0.01%	74.18%	0.00%	0.11%

TABLE V. The decompositions of the total effective coupling constant for HOMO and LUMO: local-inter, nonlocal-inter, local-intra, and nonlocal-intra parts.

	HOMO	LUMO
$G_{\text{local-inter}}$	0.103	0.095
$G_{\text{nonlocal-inter}}$	0.569	4.158
$G_{\text{local-intra}}$	0.260	0.529
$G_{\text{nonlocal-intra}}$	0.024	0.101

The results are in good agreement with the experiment which shows the band-hopping transition for electrons in naphthalene c' direction.[13]

Now, we come to the contributions of local part, nonlocal-inter part, and nonlocal-intra part to mobility at a fixed temperature. As far as the phonon contribution is concerned, apart from a common factor

$$\int_{-\infty}^{\infty} dt e^{\Sigma_\lambda -2G_\lambda(1+2N_\lambda(T))(1-\cos\,\omega_\lambda t)-\Gamma^2 t^2} \cos\left(\sum_\lambda 2G_\lambda \sin\,\omega_\lambda t\right),$$

the rest of the contribution is determined by its occupation numbers and the nonlocal coupling constants [see Eq. (3)]. From Table II, we can see that the occupation numbers of the (high frequency) intramolecular phonons are much smaller than the (low frequency) intermolecular modes. From Table V, we can see that for the nonlocal electron-phonon coupling, the intramolecular vibration is much more important than the intramolecular modes. Therefore, the intramolecule phonons are not important to the temperature dependence of mobility in all the directions. The band-hopping transition mainly resulted from the intermolecular vibrations (see Table IV).

From Table V, we can find that the intramolecular vibrations give 29.67% (12.90%) contribution to the total HOMO (LUMO) coupling constant G_{tot}. Since the major dependence of mobility on the G_{tot} is an exponential decay function [see Eq. (2)], therefore the intramolecular vibrations tend to decrease the mobility about a few tens of percents. To be more specific, we also calculate the mobility by neglecting the intramolecular modes. The ratio of total mobility and the one without intramodes are plotted in Fig. 7 as a function of temperature. As shown in Fig. 7, a reduction of about 69.1%–79.7% for electrons and 42.0%–48.4% for holes has been observed from 10 to 300 K. The reduced amounts for electrons are larger than for holes since the nonlocal electron-phonon coupling constants of electrons are larger than those of holes (see Table I and Fig. 2).

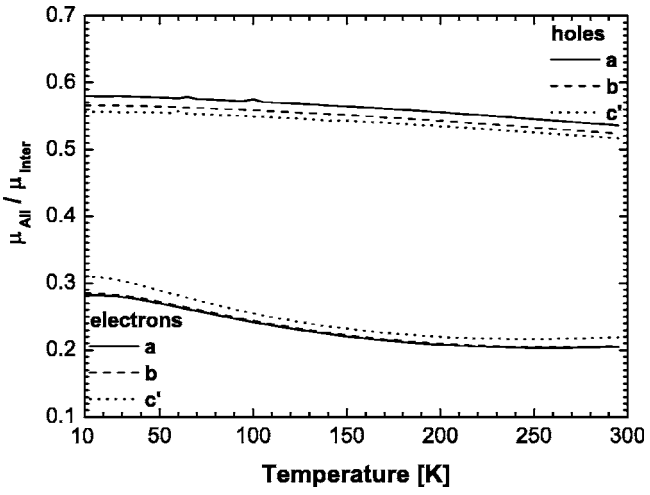

FIG. 7. The ratio between the calculated mobilities with all the phonons and the mobilities with only the intermolecular vibrations as a function of temperature for holes and electrons. (The top three curves are for holes and the rest are for electrons.)

IV. CONCLUSION

In summary, by performing a first-principles calculation for naphthalene crystals, we have investigated the band-hopping crossover and the intramolecular vibration effect which is often neglected in the carrier transport in organic crystals. We have presented a comprehensive study of the roles of inter- and intramolecular vibrations as well as the local and nonlocal electron-phonon coupling constants in the mobility anisotropy and band-hopping transition in naphthalene single crystal. Due to the small phonon occupation number and the small nonlocal coupling, the intramolecular vibrations have negligible contribution to the temperature dependence as well as to the band-hopping transition. However, they cannot be omitted in a more general and accurate theory due to their coupling with charge carriers. The intermolecular couplings are proved to be the main contribution to the T dependent charge transfer properties in naphthalene crystal.

ACKNOWLEDGMENTS

The authors are indebted to Professor Peter Bobbert for many insightful communications through email. This work is supported by the Ministry of Science and Technology of China through the 973 Program (Grant Nos. 2002CB613406 and 2006CB806200), NSFC (Grant Nos. 10425420, 20433070, and 90503013), as well as the European Union project MODECOM. The numerical calculation is performed at the Supercomputing Center of the Chinese Academy of Sciences.

[1] M. Pope and C. E. Swenberg, *Electronic Processes in Organic Crystals and Polymers*, 2nd ed. (Oxford University Press, Oxford, 1999), pp. 337–340.
[2] C. D. Dimitrakopoulos and P. R. L. Malenfant, Adv. Mater. (Weinheim, Ger.) **14**, 99 (2002).
[3] J. R. Sheats, J. Mater. Res. **19**, 1974 (2004).
[4] M. E. Gershenson, V. Podzorov, and A. F. Morpurgo, Rev. Mod. Phys. **78**, 973 (2006).
[5] T. Holstein, Ann. Phys. (N.Y.) **8**, 343 (1959).
[6] R. W. Munn and R. Silbey, J. Chem. Phys. **83**, 1854 (1985).
[7] V. M. Kenkre, J. D. Anderson, D. H. Dunlap, and C. B. Duck, Phys. Rev. Lett. **62**, 1165 (1989).
[8] K. Hannewald and P. A. Bobbert, Appl. Phys. Lett. **85**, 1535 (2004).
[9] R. A. Marcus, J. Chem. Phys. **24**, 966 (1956).
[10] N. S. Hush, Trans. Faraday Soc. **57**, 557 (1961).
[11] J. Jortner, J. Chem. Phys. **64**, 4860 (1976).
[12] A. Troisi and G. Orlandi, J. Phys. Chem. A **110**, 4065 (2006).
[13] L. B. Schein, C. B. Duck, and A. R. McGhie, Phys. Rev. Lett. **40**, 197 (1978).
[14] T. Kato and T. Yamabe, J. Chem. Phys. **115**, 8592 (2001).
[15] N. Karl, Synth. Met. **133**, 649 (2003).
[16] Y. C. Cheng, R. J. Silbey, D. A. da Silva Filho, J. P. Calbert, J. Cornil, and J. L. Brédas, J. Chem. Phys. **118**, 3764 (2003).

[17] K. Hannewald and P. A. Bobbert, Phys. Rev. B **69**, 075212 (2004).
[18] W. Q. Deng and W. A. Goddard III, J. Phys. Chem. B **108**, 8614 (2004).
[19] K. Hummer and C. Ambrosch-Draxl, Phys. Rev. B **72**, 205205 (2005).
[20] K. Hannewald, V. M. Stojanović, J. M. T. Schellekens, and P. A. Bobbert, Phys. Rev. B **69**, 075211 (2004).
[21] G. D. Mahan, *Many-Particle Physics* (Plenum, London, 1990).
[22] J. L. Brédas, D. Beljonne, V. Coropceanu, and J. Cornil, Chem. Rev. (Washington, D.C.) **104**, 4971 (2004).
[23] E. F. Valeev, V. Coropceanu, D. A. da Silva Filho, S. Salman, and J. L. Brédas, J. Am. Chem. Soc. **128**, 9882 (2006).
[24] T. Fujita, H. Nakai, and H. Nakatsuji, J. Chem. Phys. **104**, 2410 (1996).
[25] A. Troisi and G. Orlandi, Chem. Phys. Lett. **344**, 509 (2001).
[26] (a) S. W. Yin, Y. P. Yi, Q. X. Li, G. Yu, Y. Q. Liu, and Z. Shuai, J. Phys. Chem. A **110**, 7138 (2006); (b) X. D. Yang Q. K. Li, and Z. Shuai, Nanotechnology (to be published).
[27] K. Senthilkumar, F. C. Grozema, C. F. Guerra, F. M. Bickelhaupt, F. D. Lewis, Y. A. Berlin, M. A. Ratner, and L. D. A. Siebbeles, J. Am. Chem. Soc. **127**, 14894 (2005).
[28] G. Kresse and J. Hafner, Phys. Rev. B **47**, 558 (1993); **49**, 14251 (1994); G. Kresse and J. Furthmüller, *ibid.* **54**, 11169 (1996).
[29] Y. L. Page and P. Saxe, Phys. Rev. B **65**, 104104 (2002).
[30] J. P. Perdew, K. Burke, and M. Ernzerhof, Phys. Rev. Lett. **77**, 3865 (1996).
[31] E. F. C. Byrd, G. E. Scuseria, and C. F. Chabalowski, J. Phys. Chem. B **108**, 13100 (2004).
[32] V. I. Ponomarev, O. S. Filipenko, and L. O. Atovmyan, Crystallogr. Rep. **21**, 392 (1976).
[33] L. Giuggioli, J. D. Andersen, and V. M. Kenkre, Phys. Rev. B **67**, 045110 (2003).
[34] N. Karl, in *Organic Semiconductors*, Landolt Bornstein, New Series (Springer, Berlin, 1985), Group III, Vol. 17, edited by K.-H. Hellwege and O. Madelung pp. 106–218.
[35] W. Warta and N. Karl, Phys. Rev. B **32**, 1172 (1985).
[36] V. Coropceanu, J. Cornil, D. A. da Silva Filho, Y. Olivier, R. Silbey, and J. L. Brédas, Chem. Rev. **107**, 926 (2007).
[37] R. Silbey and R. W. Munn, J. Chem. Phys. **72**, 2763 (1980).